



Science Arts & Métiers (SAM)

is an open access repository that collects the work of Arts et Métiers Institute of Technology researchers and makes it freely available over the web where possible.

This is an author-deposited version published in: <https://sam.ensam.eu>
Handle ID: <http://hdl.handle.net/10985/20598>

To cite this version :

Julie CHOISNE, Christophe TRAVERT, Jean-Marc VALIADIS, Hélène FOLLET, Wafa SKALLI - A New Method To Determine Volumetric Bone Mineral Density From Bi-Planar Dual Energy Radiographs Using A Finite Element Model: An Ex-Vivo Study - Journal of Musculoskeletal Research - Vol. 20, n°03, p.1750003 - 2017

Any correspondence concerning this service should be sent to the repository

Administrator : archiveouverte@ensam.eu



Journal of Musculoskeletal Research

A New Method to Determine Volumetric Bone Mineral Density from Bi-Planar Dual Energy Radiographs Using a Finite Element Model: an Ex-Vivo Study

--Manuscript Draft--

Manuscript Number:	
Full Title:	A New Method to Determine Volumetric Bone Mineral Density from Bi-Planar Dual Energy Radiographs Using a Finite Element Model: an Ex-Vivo Study
Article Type:	Research Paper
Keywords:	Osteoporosis; bone mineral density; vertebral strength; bi-planar dual energy X-ray absorptiometry; finite element model
Corresponding Author:	Julie Choisne, Ph.D. Ecole National Superieur des Arts et Metiers Paris, FRANCE
Corresponding Author Secondary Information:	
Corresponding Author's Institution:	Ecole National Superieur des Arts et Metiers
Corresponding Author's Secondary Institution:	
First Author:	Julie Choisne, Ph.D.
First Author Secondary Information:	
Order of Authors:	Julie Choisne, Ph.D. Christophe Travert, Ph.D. Jean-Marc Valiadis, MD Helene Follet, Ph.D. Wafa Skalli, Ph.D.
Order of Authors Secondary Information:	
Manuscript Region of Origin:	FRANCE
Abstract:	<p>Finite element models (FEM) derived from QCT-scans were developed to evaluate vertebral strength but QCT scanners limitations are restrictive for routine osteoporotic diagnosis. A new approach considers using bi-planar dual energy (BP2E) X-rays absorptiometry to build vertebral FEM. The purpose was to propose a FEM based on BP2E absorptiometry and to compare the vertebral strength predicted from this model to a QCT-based FEM. Forty six vertebrae were QCT scanned and imaged with BP2E X-rays. Subject-specific vertebral geometry and bone material properties were obtained from both medical imaging techniques to build FEM for each vertebra. Vertebral body volumetric bone mineral density (vBMD) distribution and vertebral strength prediction from the BP2E-based FEM and the QCT-based FEM were compared. A statistical error of 7 mg/cm³ with a RMSE of 9.6% and a R² of 0.83 were found in the vBMD distribution differences between the BP2E-based and qCT-based FEM. The average vertebral strength was 3321N ±1657 and 3768N ±1660 for the qCT-based and BP2E-based FEM respectively with a RMSE of 641N and R² of 0.92. This method was developed to estimate vBMD distribution in lumbar vertebrae from a pair of 2D-BMD images and demonstrated to be accurate to personalize the mechanical properties in vitro.</p>

↓

**A New Method to Determine Volumetric Bone Mineral Density from Bi-Planar Dual
Energy Radiographs Using a Finite Element Model: an Ex-Vivo Study**

Julie Choisne¹ (PhD), Christophe Travert¹ (PhD), Jean-Marc Valiadis¹ (MS, MD), H el ene
Follet^{2,3} (PhD), Wafa Skalli¹ (PhD)

¹Arts et Metiers ParisTech, LBM/Institut de Biomecanique Humaine Georges Charpak, Paris,
France.

² INSERM, UMR 1033, 69008 Lyon, France

³ Universit e de Lyon, UMR 1033, 69008 Lyon, France

Corresponding Author:

Julie Choisne, PhD / Wafa Skalli, PhD

LBM/Institut de biom ecanique humaine Georges Charpak

151 boulevard de l'h opital

75013 Paris, France

Phone : (+33) 1 44 24 63 63

E-mail : jchoi005@odu.edu / wafa.skalli@ensam.eu

Short title: VBMD Estimation from BP2E radiographs

1 **Abstract**

2 Finite element models (FEM) derived from QCT-scans were developed to evaluate vertebral
3 strength but QCT scanners limitations are restrictive for routine osteoporotic diagnosis. A new
4 approach considers using bi-planar dual energy (BP2E) X-rays absorptiometry to build vertebral
5 FEM. The purpose was to propose a FEM based on BP2E absorptiometry and to compare the
6 vertebral strength predicted from this model to a QCT-based FEM. Forty six vertebrae were QCT
7 scanned and imaged with BP2E X-rays. Subject-specific vertebral geometry and bone material
8 properties were obtained from both medical imaging techniques to build FEM for each vertebra.
9 Vertebral body volumetric bone mineral density (vBMD) distribution and vertebral strength
10 prediction from the BP2E-based FEM and the QCT-based FEM were compared. A statistical error
11 of 7 mg/cm^3 with a RMSE of 9.6% and a R^2 of 0.83 were found in the vBMD distribution
12 differences between the BP2E-based and qCT-based FEM. The average vertebral strength was
13 $3321\text{N} \pm 1657$ and $3768\text{N} \pm 1660$ for the qCT-based and BP2E-based FEM respectively with a
14 RMSE of 641N and R^2 of 0.92. This method was developed to estimate vBMD distribution in
15 lumbar vertebrae from a pair of 2D-BMD images and demonstrated to be accurate to personalize
16 the mechanical properties *in vitro*.

17

18 Keywords: Osteoporosis, bone mineral density, vertebral strength, bi-planar dual energy X-ray
19 absorptiometry, finite element model

20 **1. Introduction**

21 Vertebral fractures are one of the most common clinical manifestations with the major adverse
22 consequences of osteoporosis [9, 18]. Associated with pain, disability, mortality and impairment
23 in the quality of life osteoporotic vertebral fractures affect 1.1% of women each year and 0.6% of
24 men [3, 19]. Early diagnosis of patients with osteoporosis is essential to prevent vertebral fracture.
25 However current diagnosis technique, such as dual-energy X-ray absorptiometry (DXA), can only
26 predict 40 to 70 % of vertebral fractures [24]. Such method measures areal bone mineral density
27 (aBMD) alone which does not account for vertebral geometry or the three dimensional (3D)
28 distribution of the trabecular bone. One approach for improving fracture risk assessment is to
29 estimate vertebral strength through Finite Element (FE) models with 3D geometry and mechanical
30 properties derived from quantitative computed tomography (QCT) imaging [4, 6, 13, 21]. QCT-
31 based FE models demonstrated good reliability in the vertebral strength prediction compared to *in*
32 *vitro* experiments [4-6, 13, 16, 21] and demonstrated better results than DXA to prospectively
33 assess the risk of new vertebral fractures in elderly men [27]. However, the main limitation of such
34 approach in routine osteoporotic diagnosis is the high dose, time and cost of QCT-scanner.
35 Alternative approach considers using low dose bi-planar dual energy (BP2E) X-rays
36 absorptiometry to estimate volumetric Bone Mineral Density (vBMD) from aBMD images to
37 implement in a FE model. This system allows for 3D reconstruction of the spine geometry [12]
38 and measures aBMD in the sagittal and frontal plane [23] in a 2-minutes clinical examination.
39 The purpose of this study was to propose a FE model based on bi-planar dual energy
40 absorptiometry and to compare the vertebral strength estimated from this model to a QCT-based
41 FE model which is considered as a gold standard.

42 **2. Material and methods**

43 **2.1 Specimens**

44 Human bone samples were obtained from French body donation to science program (Laboratory
45 of Anatomy, Faculty of Medicine Lyon Est, University of Lyon, France and Faculty of Medicine,
46 Centre du don des corps, University Paris Descartes, France).

47 Fourteen lumbar spine segments from cadaveric specimens were considered in this study (9
48 females and 5 males, age 84 ± 9 years). Donors were fresh cadavers and no exclusion criteria was
49 specified. A total of 46 vertebrae were included (10 L1, 12 L2, 11 L3, 11 L4 and 2 L5), after
50 exclusion of vertebrae anomalies found during radiological measurements and dissection
51 (presence of particularly severe osteophytes, disc calcifications and previous vertebral fractures).

52 **2.2 Data acquisition**

53 QCT-scans of the vertebrae were performed on two systems depending on the origin of the spine
54 sample. Eighteen vertebrae were scanned on a QCT machine (MX8000 IDT10, Philips Medical,
55 Best, Netherlands), using the following settings; X-ray tube voltage and current: 120kV, 100mA,
56 reconstruction matrix: 512×512 , field of view: 250×250 mm, voxel size of $0.48 \times 0.48 \times 1$ mm. They
57 were scanned alongside a K₂HPO₄ phantom (Mindways, Austin, TX, USA). The remaining
58 vertebrae were scanned on a Scanner ICT 256 (Philips Healthcare, Cleveland, OH, USA) with the
59 following settings; X-ray tube voltage and current: 120kV, 1489mA/s, reconstruction matrix:
60 512×512 , field of view: 250×250 mm, voxel size of $0.39 \times 0.39 \times 0.33$ mm. A calibration phantom
61 (QRM-ESP, QRM GmbH, Germany) was used to map gray scale values to bone mineral density.
62 To ensure consistency between the different protocols and have a cross-calibration, the Mindways
63 phantom was scanned alongside the European Spine Phantom to determine the HA concentration
64 equivalent for the different parts of the Mindways phantom. Similar calibration was thus
65 performed on the QCT images to measure vBMD in each vertebra.

66 Low dose bi-planar dual energy (BP2E) X-rays were acquired for all spine segments using a dual
67 energy prototype of the EOS® system (EOS imaging, Paris, France) which can simultaneously
68 take a pair of X-rays in the sagittal and frontal planes in upright position [8], allowing 3D
69 reconstruction of the spine [12]. Two levels of energy can be achieved with the EOS prototype by
70 quickly changing the X-ray tube settings between two fast scans (approximately 20 seconds
71 depending on the size of the lumbar spine). Therefore the computed projected areal Bone Mineral
72 Density (aBMD) images of the vertebrae are similar to DXA images [21, 23]. ABMD
73 measurement was previously validated by comparing EOS accuracy and reproducibility with the
74 dual x-ray absorptiometry densitometers' characteristics [23]. X-ray tube voltage and current were
75 140kV and 149mA for the high energy images and 70kV and 298mA for the low energy images.

76 **2.3 Finite Element Models**

77 A QCT-based finite element (FE) model was built from vertebral geometry obtained by a semi-
78 automatic segmentation method [15]. A hexahedral mesh of the vertebra was generated from this
79 geometry using a multiblock meshing program wrote in C++ [10]. Briefly, the multiblock meshing
80 technique consists in multiple building blocks composed of meshing seeding arranged in rows,
81 columns and layers. The mesh seeds are then projected on the vertebra surface and morphed to
82 each vertebral surface as nodes to lay the foundation for the FE mesh [10], resulting to a different
83 topology for each vertebral level. In this 17,000-element mesh the average element size was
84 controlled to range between 1 mm and 1.5 mm. All FE meshes were generated with the same
85 topology for each lumbar level allowing the same element to be located closely at the same position
86 for each vertebra at the same lumbar level. Convergence analysis was performed to determine the
87 ideal number of elements needed [26]. Once the mesh generated, the average BMD of a single
88 finite element was defined on the basis of the QCT scan voxels that fall inside the element. A

89 volumetric BMD (vBMD) distribution was defined as the set of density values of each element of
90 a model. As elements correspond to their counterpart in the same level vertebra mesh instances,
91 comparison between vBMD distributions on element per element basis was feasible. Finally,
92 vBMD values of the elements were converted to linear elastic mechanical properties from an
93 experimental relationship between vBMD and elastic modulus [14] as shown in equation 1.

$$94 \quad E \text{ (MPa)} = 3230 \text{ BMD (gHA/cm}^3\text{)} - 34.7 \quad (1)$$

95 The Poisson ratio, ν , was set to 0.4 [13].

96 A bi-planar dual energy based (BP2E-based) FE model was built from vertebral geometry obtained
97 by 3D reconstruction of the spine from bi-planar X-rays [12]. By using calibrated sagittal and
98 frontal X-ray images we were able to reconstruct a patient-specific geometry of each vertebrae.
99 FE meshes similar to the QCT-based model were generated using the same element numbering
100 and topology.

101 The vBMD distribution was estimated for each mesh from the sagittal and/or frontal areal BMD
102 (aBMD) images and a generic vBMD distribution, using the algorithm described in the following
103 section. Finally, vBMD values were converted to material properties using the same equation 1.

104 **2.4 vBMD distribution estimation from aBMD images**

105 An algorithm was developed to estimate the vBMD distribution from bi-planar dual energy (BP2E)
106 X-ray absorptiometry images for each vertebra. The global approach is illustrated in figure 1 and
107 presented hereafter.

108 First, a database composed of the QCT-based FE mesh densities was built from the 46 vertebrae
109 distinguishing each lumbar level. The database was composed of 10 L1, 12 L2, 11 L3, 11 L4 and
110 2 L5. From this database, a generic vBMD distribution was created by averaging for each single
111 finite element the density found in all vertebrae for each lumbar level. By having the same topology

112 for all vertebral meshes we can obtain an initial FE mesh pre-filled with the generic vBMD
113 distribution. Once we have an initial FE model filled with a generic vBMD distribution for a given
114 vertebra, we were able to build digitally reconstructed radiographies (DRR) yielding to virtual
115 aBMD images (frontal and sagittal views) based on the generic vBMD distribution. In this process,
116 the vertebra under control was removed from the QCT-based FE mesh density database to not
117 influence in the generic vBMD distribution. In order to personalize the vBMD distribution, these
118 virtual aBMD images were compared to the BP2E aBMD images resulting from dual energy
119 acquisition. Differences were quantified in terms of density value for each image pixel. Then, an
120 automatic iterative adjustment of the vBMD distributions was performed to minimize these
121 differences between the virtual and the BP2E aBMD images.

122 **2.5 Boundary conditions**

123 Previously described boundary conditions and failure criterion [21] were considered to compare
124 the QCT-based and BP2E-based models. Briefly, each vertebra was virtually loaded in anterior
125 compression via a thin layer of polymethyl-methacrylate (PMMA, about 0.5 to 1cm thick, $E=2500$
126 MPa, $\nu=0.3$) placed over the vertebral endplates as performed previously [21]. Lower nodes of the
127 lower PMMA layer were constrained in all degrees of freedom. Anterior compressive load was
128 applied to a node located at the anterior third of the vertebra joined by rigid elements to the upper
129 PMMA layer. Simulations were run on ANSYS software (ANSYS Inc., Canonsburg, PA, USA).
130 The vertebral failure load was defined when a contiguous region of 1mm^3 of elements reached
131 1.5% deformation as determined previously [21, 22].

132 **2.6 Analysis of the accuracy of the predictive vBMD**

133 The method developed to estimate the vBMD distribution from BP2E images can be affected by
134 the number of radiography used (1 sagittal or 1 frontal or both radiographies). Therefore we first

135 compared the vBMD distribution from the QCT-based model, considered as a gold standard, to
136 the BP2E-based model on 18 vertebrae with three methodologies to estimate the BP2E-based
137 vBMD from the aBMD radiographies; 1) by using the sagittal radiography only, 2) by using the
138 frontal radiography alone and 3) by using both radiographs. Once the best method was defined,
139 the 46 vertebrae were used to validate the BP2E-based FEM from the qCT-based FEM by
140 comparing the vertebral strength determined from each model.

141 In more details, one group composed of 18 vertebrae (from 5 donors, 4F and 1M, mean age: $78 \pm$
142 8 y.o.) was used to compare the vBMD distribution assessed by the QCT model to the three BP2E
143 models (depending on the radiographies used for the method; 1) the sagittal image only, 2) the
144 frontal image and 3) both frontal and sagittal BP2E images). To evaluate the vBMD estimation
145 method, the mean BMD estimated in the vertebral body trabecular bone from each model was
146 computed as the average of the inner vertebral body elements, weighted by each element volume.
147 The two outer layers of elements, corresponding to cortical bone, were removed of the comparison
148 as trabecular bone is more affected by osteoporosis than the cortical layer. Therefore the inner
149 vBMD, corresponding to the trabecular bone, based from the BP2E model were compared to the
150 average vBMD measured in the same volume on the qCT-based model. Each vertebra's centrum
151 was then divided in 27 parts bounded by two frontal planes, two axial planes and two para-sagittal
152 planes, as shown in figure 2.

153 This division of the vertebral body was performed to assess the reliability of the vBMD estimation
154 method in different regions of the trabecular bone as regional variation is present in vertebral bone
155 density [11]. Average vBMD distribution in each of the 27 regions based from the BP2E model
156 were compared to the average vBMD measured in the same regions on the qCT-based model. The
157 statistical error, the root mean square error (RMSE), Bland and Altman plots [2] and the non-

158 parametric Spearman R^2 coefficient between the vBMD estimated from each BP2E-based model
159 and the vBMD measured from qCT-scan were computed. The statistical differences between the
160 models were assessed by a Wilcoxon signed rank test ($p < 0.05$).

161 The methodology presenting the least error and the highest R^2 coefficient was then applied to
162 estimate the vBMD distribution on the BP2E-based FEM. Then, the vertebral strength calculated
163 from both FEMs was determined on the 46 vertebrae as the maximum load the vertebrae can
164 sustain before failure. Differences in vertebral strength between the BP2E-based FEM and qCT-
165 based FEM were assessed by computing the standard error of the estimate (SEE), the RMSE and
166 the parametric Pearson R^2 correlation coefficient. For both analysis the correlation coefficients
167 (R^2) were calculated both in their raw and sample size adjusted forms (adj. R^2).

168 **3. Results**

169 **3.1 Estimation of the vBMD**

170 Three methodologies to estimate the vBMD distribution from the BP2E aBMD radiographies were
171 compared to the QCT vBMD: 1) by using the sagittal radiography only, 2) by using the frontal
172 view alone and 3) by using both radiographs. Results for the three methodologies are presented in
173 Table 1 with Bland and Altman plots displayed in Figure 3.

174 The best method found to estimate the average vBMD from BP2E images with the lower RMSE
175 was using the sagittal plane image alone which led to a RMSE of 10 mg/cm^3 compared to the qCT-
176 based model. After dividing the vertebral body into 27 regions, the vBMD distribution of all
177 regions were estimated with a RMSE of 13 mg/cm^3 using the sagittal radiograph. No significant
178 vBMD distribution differences were found between the qCT-based model and the BP2E-based
179 model.

180 **3.2 Finite Element Model**

181 The BP2E-based FE model vertebral strength was calculated using the sagittal radiograph only as
182 it was established to be the method involving the lower errors in vBMD estimation. The mean
183 vertebral strength estimated by the BP2E-based FE model and the QCT-based FE model were
184 3768 N \pm 1660 and 3321 N \pm 1657 respectively. A significant correlation coefficient was found
185 between the two models with $R^2=0.92$ with $p<0.001$ (adj. $R^2=0.92$ with $p<0.001$), a RMSE of 9.6
186 % and a Standard Error of the Estimate of 461 N (Figure 4 A-B).

187 **4. Discussion**

188 **4.1 Distribution of the vBMD**

189 The purpose of this study was to propose a new method to determine vBMD from bi-planar dual
190 energy (BP2E) X-ray radiographies that could be used for osteoporotic vertebral strength
191 estimation. First the technique used to build a vBMD distribution from BP2E X-rays was assessed
192 by comparing the estimated vertebral body vBMD distribution to the measured vBMD from QCT
193 scan. Second vertebral strength estimation was evaluated using a subject-specific Finite Element
194 (FE) model built from the estimated BP2E vBMD compared to a QCT-based FE model considered
195 as a gold standard.

196 Even though the 3D geometry of the spine was obtained by 3D reconstruction from the sagittal
197 and frontal planes X-rays, three methodologies were analyzed to estimate the vBMD from the
198 BP2E radiographies; 1) using the sagittal radiography only, 2) using the frontal view alone and 3)
199 using both radiographs. Average vertebral body vBMD distribution from BP2E images showed a
200 lower RMSE compared to qCT scan when using the sagittal plane radiograph alone to estimate
201 vBMD with a 95% confidence interval (CI) of ± 20 mg/cm³. The same conclusion was drawn
202 when comparing vBMD in 27 sub-regions in the vertebral body. Using sagittal and frontal plane
203 BP2E radiographs to estimate vBMD increased the RMSE of 48%. Using the frontal radiograph

204 alone increased the RMSE of 91%. This increase in error when using the frontal plane radiograph
205 can be explained by the superimposition of the posterior arch with the vertebral body in the frontal
206 view. With a mean density of 321 mg/cm^3 at the posterior arch vs 161 mg/cm^3 for the vertebral
207 body, one can assume that the presence of the posterior elements in the frontal view can affect the
208 estimation of the vertebral body's vBMD. For the same reasons, using the frontal view in addition
209 to the sagittal view also deteriorated the average vertebral body vBMD.

210 This study is the first to report on the estimation vertebral body vBMD from the EOS BP2E X-
211 rays. Previous studies used volumetric DXA (VXA) to determine vBMD distribution in the lumbar
212 spine from L2 to L4 [29] and in the proximal femur [1, 28] and compared it with QCT vBMD. A
213 statistical shape and density model was developed for L2, L3 and L4 to estimate vBMD from
214 sagittal and frontal planes DXA images on female subjects [29]. Because this study explored VXA
215 accuracy *in vivo*, which includes soft tissue artifact, the error found were higher than the present
216 study with confidence intervals ranging from 41.2 to 51.8 mg/cm^3 in vertebral body vBMD
217 estimation versus 20 mg/cm^3 in the present study. Their finding show great promises that using
218 the EOS system *in vivo* could provide similar results. As for the femur, a 95% CI ranging from
219 40.8 mg/cm^3 to 56.2 mg/cm^3 were found in different region [28] which is higher than the present
220 study (25 mg/cm^3 for the 27 regions). Correlation coefficient between 0.81 and 0.95 for the narrow
221 neck [1] and the global proximal femur [28] were reported and the present study found correlation
222 coefficients equal to 0.84. While the results cannot be compared directly because of the differences
223 between DXA and EOS, the same range of correlations and vBMD estimation errors were found,
224 which is encouraging for further study.

225 **4.2 Finite Element Models**

226 Vertebral strength estimation was also evaluated using a Finite Element (FEM) model built from
227 the estimated BP2E vBMD compared to the QCT-based FEM. Some studies assessed vertebral
228 strength prediction using a FE model based on QCT imaging [4-6, 13, 16]. The predicted ultimate
229 force was well correlated with *in vitro* experiments with squared correlation coefficients ranging
230 from 0.77 [5] to 0.95 [13]. Average reported vertebral strength varied between 2979 N to 5391 N
231 which is in the range of the present results based on the qCT-based FEM (3321 N) and BP2E-
232 based FEM (3768 N). A high significant squared correlation coefficient between the two models
233 was found with a slope of 0.96 and an offset of 446 N meaning that the BP2E based model is a
234 good predictor for vertebral strength estimation compared to the QCT-based FEM. One of the
235 limitation is, the QCT-based FE model strength prediction accuracy was not examined with
236 mechanically measured strength as *in vitro* experiments were not performed in the present study.
237 However QCT based FEM is now a well-established method to determine vertebral strength [4-6,
238 13, 16], with future study will examine the accuracy of the models in estimating *in vitro* vertebral
239 strength. Compared to DXA, which is the most used clinical tool to detect osteoporosis, FE models
240 are more capable to predict vertebral strength. When considering *in vivo* study [27], DXA was
241 fairly correlated to vertebral strength predicted from QCT-models with a correlation coefficient of
242 0.79. Moreover, FE strength was the most robust predictor for vertebral fracture prognostic
243 compared to DXA. Therefore, FE models based on medical imaging would significantly help in
244 predicting vertebral fractures. While QCT-based models present lots of advantages with
245 volumetric geometry and BMD, they are also costly with high radiation dose required for
246 moderately high-resolution. The present study could propose an alternative to the qCT scan
247 disadvantages keeping volumetric geometry and BMD estimation possible. Indeed the EOS device
248 is a low dose X-ray system with a fast acquisition time and an effective dose received of ~0.3 mSv

249 [7] compared to 5 mSv with qCT scan [27]. Sagittal and frontal DXA images were used with the
250 same approach [1, 17, 20, 25, 30], however DXA images resolution is low with a high
251 reproducibility error [1, 23, 28, 29] and the EOS system takes X-ray in a standing position so that
252 postural influence on vertebral fracture can be assessed.

253 Provided the present model gives as good results *in vivo*, it would be a good alternative to QCT-
254 based FE models. Several limitations are still to be considered. Possible error sources were the
255 accuracy of the 3D reconstruction, which can affect the vertebral body volume and thus the
256 apparent density, the contribution of the cortical bone layer and, to a lesser extent, the surrounding
257 soft tissues. However, spine 3D reconstruction position precision was quantified to be less than
258 1.8 mm which should not affect average vBMD distribution [12]. Reproducibility of the volumetric
259 BMD distribution from the EOS system was not assessed in the present study but areal BMD
260 accuracy of the EOS system was determined to be below 5.2 per cent, versus 7.2 per cent for a
261 DXA system in the same conditions [23]. As the transformation from aBMD into vBMD
262 distribution is completely automated, we can assume that the accuracy will be similar than for the
263 EOS aBMD. Cortical shell was not modeled in either FEMs since qCT-scan is not precise enough
264 to measure cortical thickness with voxel sizes being larger than average cortical thickness in a
265 vertebra. The influence of neglecting the cortical shell was not quantified in the present study but
266 should be considered in future study including micro-CT imaging of the vertebrae. Thoracic
267 vertebrae are also a concern for osteoporotic fractures, however L1 to L4 are easily measured in
268 dual energy absorptiometry because of no superimposition of the thoracic cage or pelvis on the
269 images.

270 Future studies should validate this model with *in vitro* experiments. The present study considered
271 QCT-based FE models as gold standard but the literature [4-6, 13, 16] showed that an average

272 error ranging from 275 N to 1338 N can occur when comparing *in vitro* vertebral strength to QCT-
273 based FE models predicted strength. Then the model should be validated *in vivo* considering soft
274 tissue attenuation. Soft tissue characterization from the frontal view will allow for *in vivo*
275 application.

276 This methodology was developed to estimate vBMD distribution in lumbar vertebrae from a pair
277 of dual energy absorptiometry EOS images. This method is accurate enough and sufficient to
278 personalize the mechanical properties in a FE model for vertebral strength estimation. Once these
279 results are confirmed *in vivo*, FE models based on low dose bi-planar dual energy EOS images
280 could become an alternative to QCT-based FEM.

281 **Disclosures**

282 The authors have no conflict of interest to declare. Wafa Skalli is the co-inventor of the EOS
283 system without direct financial interest.

284 **Acknowledgments**

285 The authors would like to thank N. Vilayphiou, J.B. Pialat and F. Duboeuf for contributing to
286 image acquisition. The authors would also thank Anabela Darbon, advanced research engineer at
287 EOS Imaging, for EOS dual energy acquisition and calibration.

288 **Submission statement**

289 We represent that this submission is original work, and is not under consideration for publication
290 with any other journal

291 **References**

- 292 1. Ahmad O, Ramamurthi K, Wilson KE, Engelke K, Prince RL, and Taylor RH. Volumetric
293 DXA (VXA): A new method to extract 3D information from multiple *in vivo* DXA images.
294 *J Bone Miner Res* **25**(12): 2744-51, 2010

- 295 2. Bland JM and Altman DG. Statistical methods for assessing agreement between two
296 methods of clinical measurement. *Lancet* **1**(8476): 307-10, 1986
- 297 3. Bliuc D, Nguyen ND, Milch VE, Nguyen TV, Eisman JA, and Center JR. Mortality risk
298 associated with low-trauma osteoporotic fracture and subsequent fracture in men and
299 women. *JAMA* **301**(5): 513-21, 2009
- 300 4. Buckley JM, Loo K, and Motherway J. Comparison of quantitative computed tomography-
301 based measures in predicting vertebral compressive strength. *Bone* **40**(3): 767-774, 2007
- 302 5. Chevalier Y, Charlebois M, Pahr D, Varga P, Heini P, Schneider E, and Zysset P. A patient-
303 specific finite element methodology to predict damage accumulation in vertebral bodies
304 under axial compression, sagittal flexion and combined loads. *Computer Methods in*
305 *Biomechanics and Biomedical Engineering* **11**(5): 477-487, 2008
- 306 6. Crawford RP, Cann CE, and Keaveny TM. Finite element models predict in vitro vertebral
307 body compressive strength better than quantitative computed tomography. *Bone* **33**(4):
308 744-750, 2003
- 309 7. Damet J, Fournier P, Monnin P, Sans-Merce M, Ceroni D, Zand T, Verdun FR, and
310 Baechler S. Occupational and patient exposure as well as image quality for full spine
311 examinations with the EOS imaging system. *Medical Physics* **41**(6), 2014
- 312 8. Dubousset J, Charpak G, Skalli W, Deguise J, and Kalifa G. EOS: A new imaging system
313 with low dose radiation in standing position for spine and bone & joint disorders. *Journal*
314 *of Musculoskeletal Research* **13**(1): 1-12, 2010
- 315 9. Ettinger B, Black DM, Nevitt MC, Rundle AC, Cauley JA, Cummings SR, and Genant
316 HK. Contribution of vertebral deformities to chronic back pain and disability. The Study
317 of Osteoporotic Fractures Research Group. *J Bone Miner Res* **7**(4): 449-56, 1992

- 318 10. Grosland NM, Shivanna KH, Magnotta VA, Kallemeyn NA, DeVries NA, Tadepalli SC,
319 and Lisle C. IA-FEMesh: an open-source, interactive, multiblock approach to anatomic
320 finite element model development. *Comput Methods Programs Biomed* **94**(1): 96-107,
321 2009
- 322 11. Hulme PA, Boyd SK, and Ferguson SJ. Regional variation in vertebral bone morphology
323 and its contribution to vertebral fracture strength. *Bone* **41**(6): 946-957, 2007
- 324 12. Humbert L, De Guise JA, Aubert B, Godbout B, and Skalli W. 3D reconstruction of the
325 spine from biplanar X-rays using parametric models based on transversal and longitudinal
326 inferences. *Medical Engineering and Physics* **31**(6): 681-687, 2009
- 327 13. Imai K, Ohnishi I, Bessho M, and Nakamura K. Nonlinear finite element model predicts
328 vertebral bone strength and fracture site. *Spine (Phila Pa 1976)* **31**(16): 1789-94, 2006
- 329 14. Kopperdahl DL, Morgan EF, and Keaveny TM. Quantitative computed tomography
330 estimates of the mechanical properties of human vertebral trabecular bone. *J Orthop Res*
331 **20**(4): 801-5, 2002
- 332 15. Le Pennec G, Campana S, Jolivet E, Vital JM, Barreau X, and Skalli W. CT-based semi-
333 automatic quantification of vertebral fracture restoration. *Computer Methods in*
334 *Biomechanics and Biomedical Engineering* **17**(10): 1086-1095, 2014
- 335 16. Liebschner MA, Kopperdahl DL, Rosenberg WS, and Keaveny TM. Finite element
336 modeling of the human thoracolumbar spine. *Spine (Phila Pa 1976)* **28**(6): 559-65, 2003
- 337 17. López E, Casajús JA, Ibarz E, Gómez-Cabello A, Ara I, Vicente-Rodríguez G, Mateo J,
338 Herrera A, and Gracia L. Application of a model based on dual-energy X-ray
339 absorptiometry and finite element simulation for predicting the probability of osteoporotic

- 340 hip fractures to a sample of people over 60 years. *Proceedings of the Institution of*
341 *Mechanical Engineers, Part H: Journal of Engineering in Medicine* **229**(5): 369-385, 2015
- 342 18. O'Neill TW, Cockerill W, Matthis C, Raspe HH, Lunt M, Cooper C, Banzer D, Cannata
343 JB, Naves M, Felsch B, Felsenberg D, Janott J, Johnell O, Kanis JA, Kragl G, Lopes Vaz
344 A, Lyritis G, Masaryk P, Poor G, Reid DM, Reisinger W, Scheidt-Nave C, Stepan JJ, Todd
345 CJ, Woolf AD, Reeve J, and Silman AJ. Back pain, disability, and radiographic vertebral
346 fracture in European women: a prospective study. *Osteoporos Int* **15**(9): 760-5, 2004
- 347 19. Oleksik A, Lips P, Dawson A, Minshall ME, Shen W, Cooper C, and Kanis J. Health-
348 related quality of life in postmenopausal women with low BMD with or without prevalent
349 vertebral fractures. *J Bone Miner Res* **15**(7): 1384-92, 2000
- 350 20. Pottecher P, Engelke K, Duchemin L, Museyko O, Moser T, Mitton D, Vicaut E, Adams
351 J, Skalli W, Laredo JD, and Bousson V. Prediction of Hip Failure Load: In Vitro Study of
352 80 Femurs Using Three Imaging Methods and Finite Element Models—The European
353 Fracture Study (EFFECT). *Radiology* **280**(3): 837-847, 2016
- 354 21. Sapin-De Brosses E, Jolivet E, Travert C, Mitton D, and Skalli W. Prediction of the
355 vertebral strength using a finite element model derived from low-dose biplanar imaging:
356 Benefits of subject-specific material properties. *Spine* **37**(3): E156-E162, 2012
- 357 22. Sapin De Brosses E, Briot K, Kolta S, Skalli W, Roux C, and Mitton D. Subject-specific
358 mechanical properties of vertebral cancellous bone assessed using a low-dose X-ray
359 device. *IRBM* **31**(3): 148-153, 2010
- 360 23. Sapin E, Briot K, Kolta S, Gravel P, Skalli W, Roux C, and Mitton D. Bone mineral density
361 assessment using the EOS low-dose X-ray device: a feasibility study. *Proc Inst Mech Eng*
362 *H* **222**(8): 1263-71, 2008

- 363 24. Sornay-Rendu E, Munoz F, Garnero P, Duboeuf F, and Delmas PD. Identification of
364 osteopenic women at high risk of fracture: the OFELY study. *J Bone Miner Res* **20**(10):
365 1813-9, 2005
- 366 25. Tatoń G, Rokita E, Wróbel A, and Korkosz M. Combining areal DXA bone mineral density
367 and vertebrae postero-anterior width improves the prediction of vertebral strength. *Skeletal*
368 *Radiology* **42**(12): 1717-1725, 2013
- 369 26. Travert. C. *Estimation du risque de fracture ostéoporotique du rachis thoraco-lombaire*
370 *par un modèle en éléments finis personnalisé*. LBM/Institut de biomécanique humaine
371 Georges Charpak, Arts et Métiers ParisTech, p. 131, 2012.
- 372 27. Wang X, Sanyal A, Cawthon PM, Palermo L, Jekir M, Christensen J, Ensrud KE,
373 Cummings SR, Orwoll E, Black DM, and Keaveny TM. Prediction of new clinical
374 vertebral fractures in elderly men using finite element analysis of CT scans. *J Bone Miner*
375 *Res* **27**(4): 808-16, 2012
- 376 28. Whitmarsh T, Humbert L, De Craene M, Del Rio Barquero LM, and Frangi AF.
377 Reconstructing the 3D shape and bone mineral density distribution of the proximal femur
378 from dual-energy X-ray absorptiometry. *IEEE Trans Med Imaging* **30**(12): 2101-14, 2011
- 379 29. Whitmarsh T, Humbert L, Del Río Barquero LM, Di Gregorio S, and Frangi AF. 3D
380 reconstruction of the lumbar vertebrae from anteroposterior and lateral dual-energy X-ray
381 absorptiometry. *Medical Image Analysis* **17**(4): 475-487, 2013
- 382 30. Yang L, Palermo L, Black DM, and Eastell R. Prediction of Incident Hip Fracture with the
383 Estimated Femoral Strength by Finite Element Analysis of DXA Scans in the Study of
384 Osteoporotic Fractures. *Journal of Bone and Mineral Research* **29**(12): 2594-2600, 2014

385 **Supporting information captions**

386 Table 1: Mean (\pm SD), Root Mean Square Error (RMSE), the Spearman R^2 coefficient and the
 387 statistical error in volumetric bone mineral density distribution (vBMD) between the QCT scan
 388 model and the bi-planar dual energy (BP2E) model in the inner vertebral body and in the 27
 389 trabecular regions as described in Figure 2 then pooled together before analysis.

vBMD (mg/cm ³)		Sagittal view	Frontal view	Sagittal and Frontal views	
Inner body	Mean (SD)	qCT	124 (50)		
		BP2E	130 (45)	170 (46)	163 (50)
	RMSE (%)		10 (9.6%)	127 (91%)	76 (48%)
	Statistical error (p value)		7 (0.058)	46 (<0.0001)	39 (<0.0001)
	R^2 (p value)		0.83(<0.0001)	0.62 (0.0001)	0.77 (<0.0001)
	Adjusted R^2		0.82	0.60	0.76
Pooled 27 sub-regions	Mean (SD)	qCT	121 (55)		
		BP2E	119 (41)	151 (37)	139 (41)
	RMSE (%)		13 (3.7%)	155 (40%)	93 (14%)
	Statistical error (p value)		-2 (0.983)	30 (0.003)	18 (0.010)
	R^2 (p value)		0.71 (<0.0001)	0.37 (<0.0001)	0.32 (0.002)
	Adjusted R^2		0.70	0.36	0.31

390
 391 Figure 1: FE model built from bi-planar dual energy (BP2E) and QCT images. The method to
 392 estimate the volumetric BMD (vBMD) distribution from BP2E images is detailed in the bolded
 393 grey square. First (1.), a vBMD distribution based on the QCT density database was used to build
 394 a generic distribution. Second (2.), a digitally reconstructed radiography (virtual aBMD image)
 395 was made based on the generic distribution from (1.). Third (3.) an iterative vBMD adjustment

396 was performed to maximize pixel similarity between the virtual and BP2E aBMD images. Once
397 the image similarity was optimized, the personalized vBMD distribution from BP2E images was
398 set.

399 Figure 2: Division of the vertebral body in 27 regions used to assess volumetric Bone Mineral
400 Density distribution errors.

401 Figure 3: Error in the average vBMD distribution estimated from bi-planar dual energy (BP2E) X-
402 ray absorptiometry radiographies compared to QCT images from the (A) the sagittal image alone,
403 (B) the frontal image alone and (C) the sagittal and frontal images. Error in each of the 27 regions
404 vBMD distribution estimated from the (D) the sagittal image alone, (E) the frontal image alone
405 and (F) the sagittal and frontal images.

406 Figure 4: A) Regression Analysis and B) Bland and Altman plot between vertebral strength
407 determined from BP2E-based FEM and qCT-based FEM. VBMD distribution estimated from the
408 sagittal image only.

Figure1

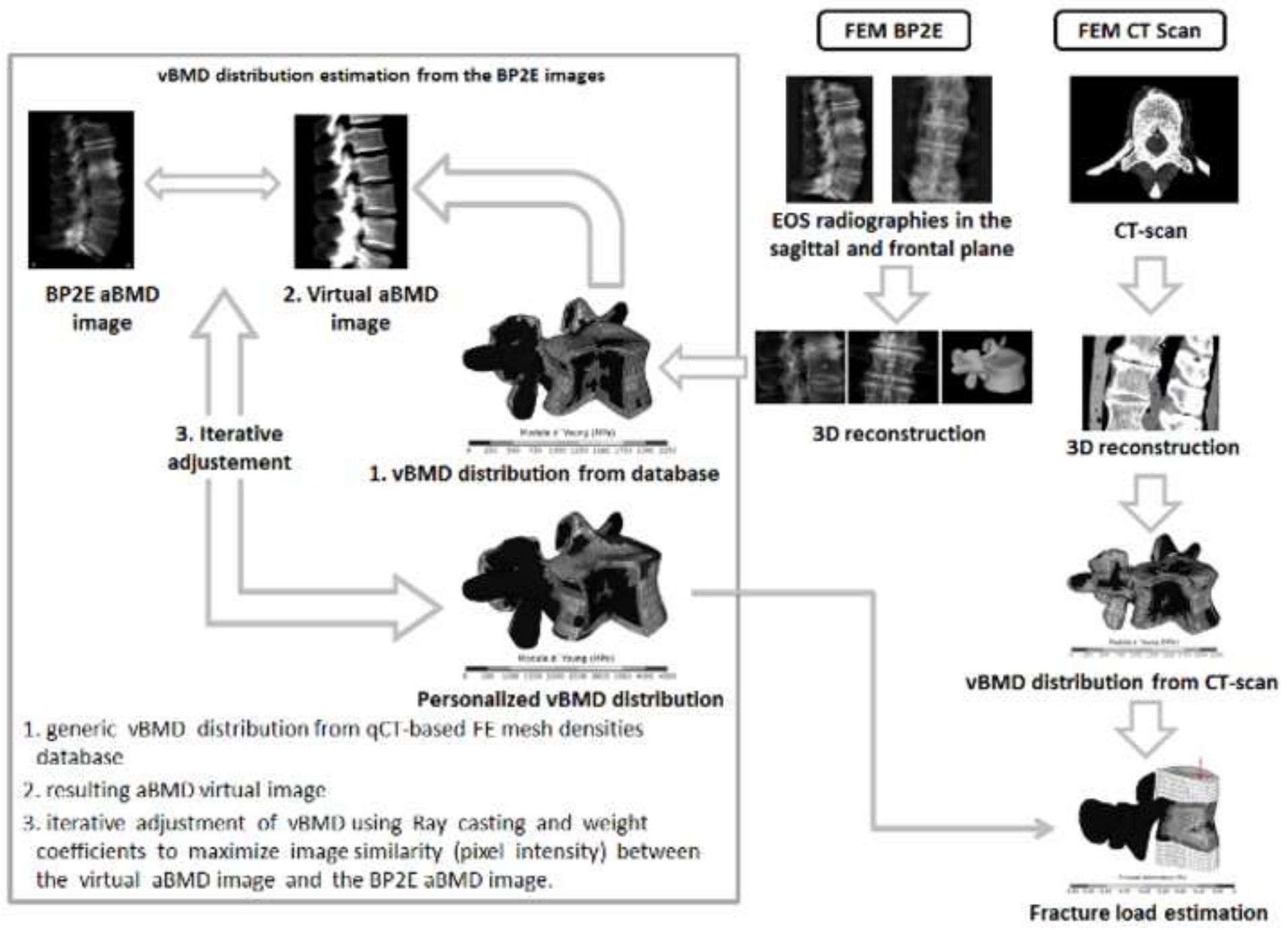


Figure2

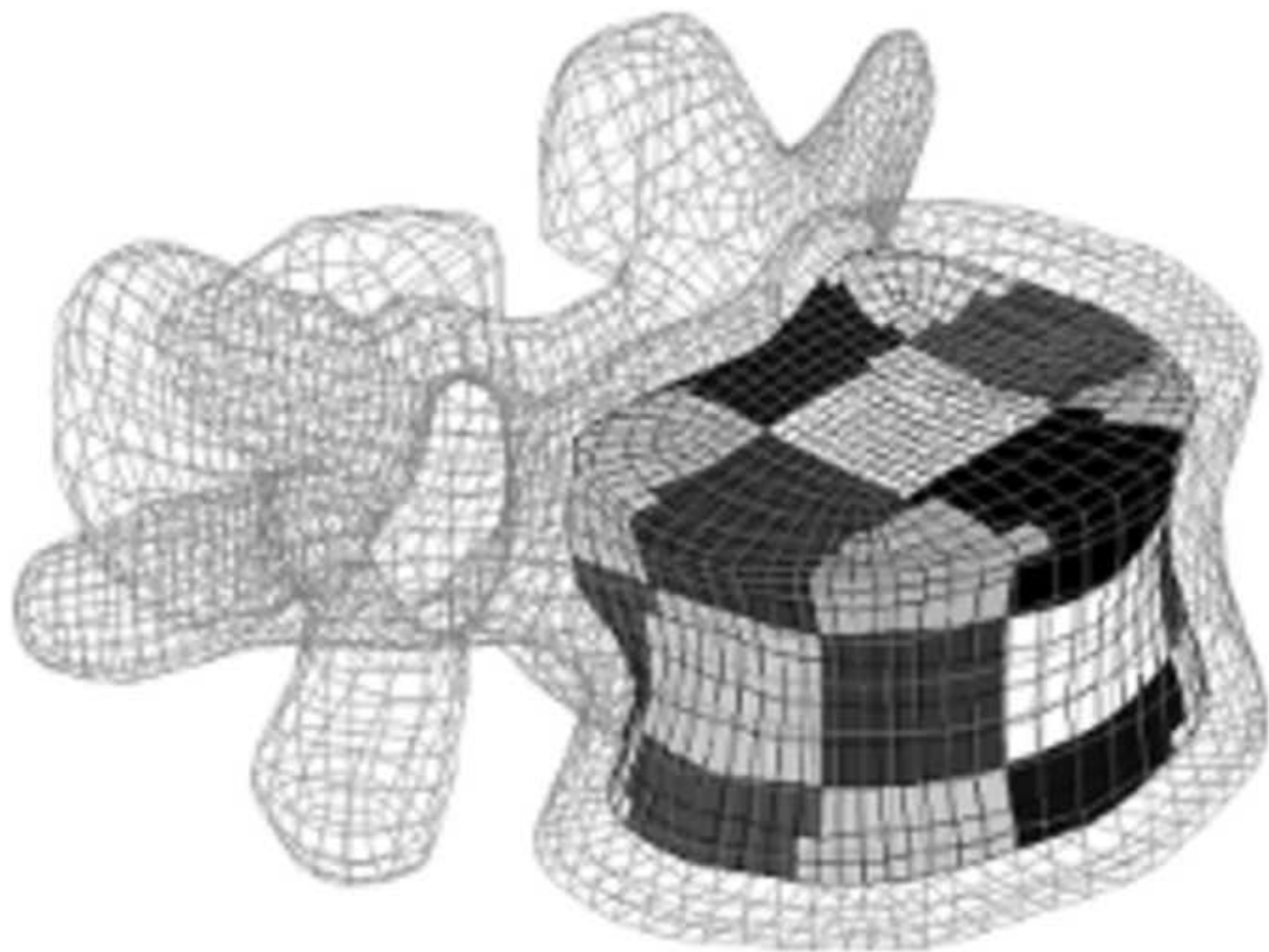


Figure 3

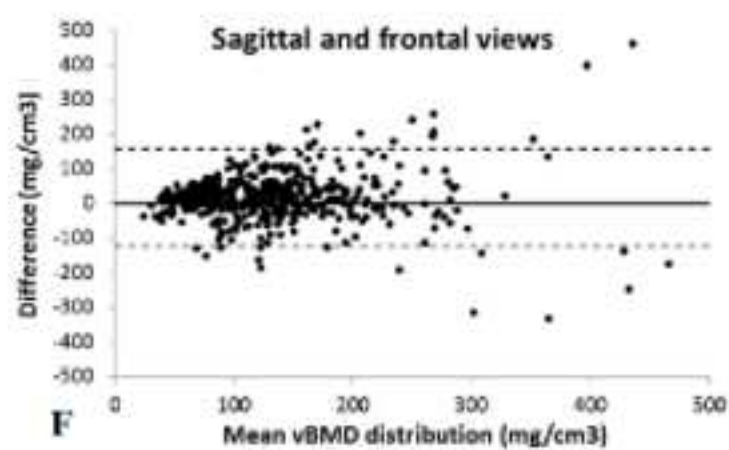
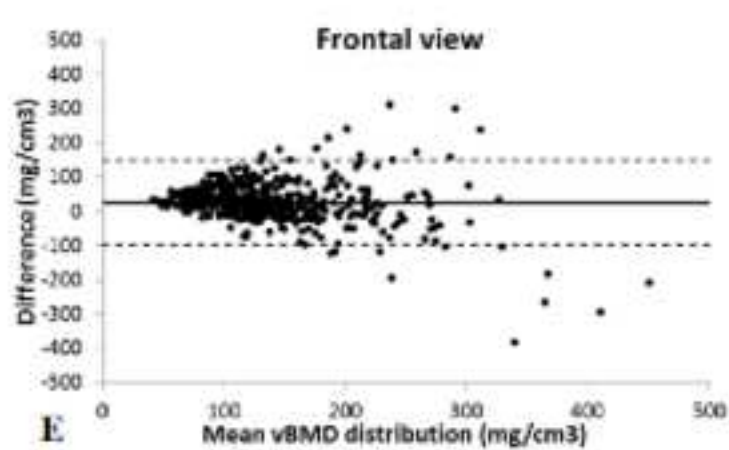
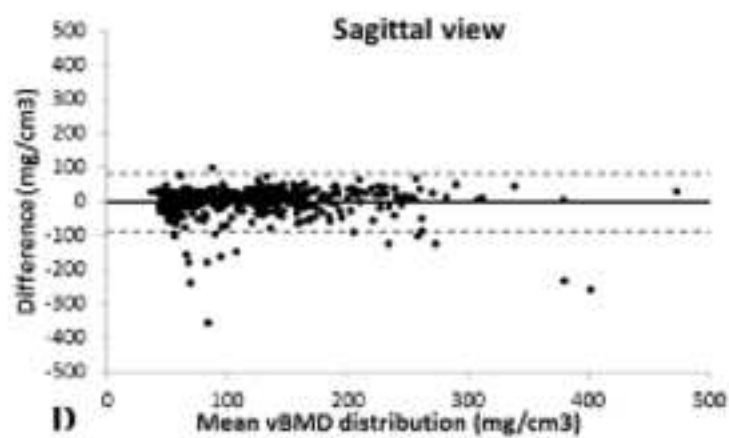
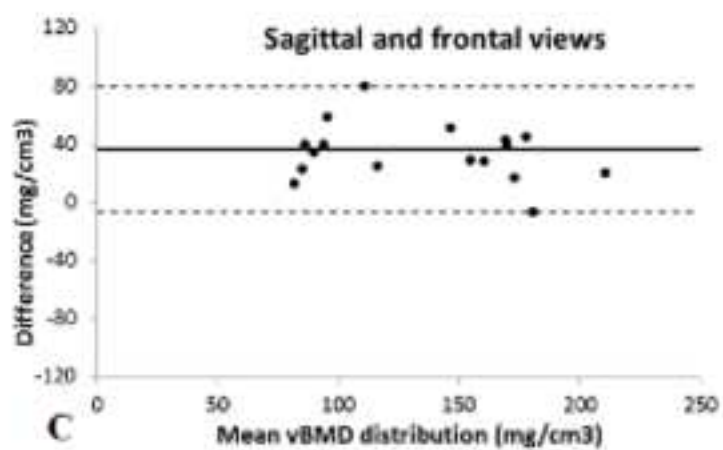
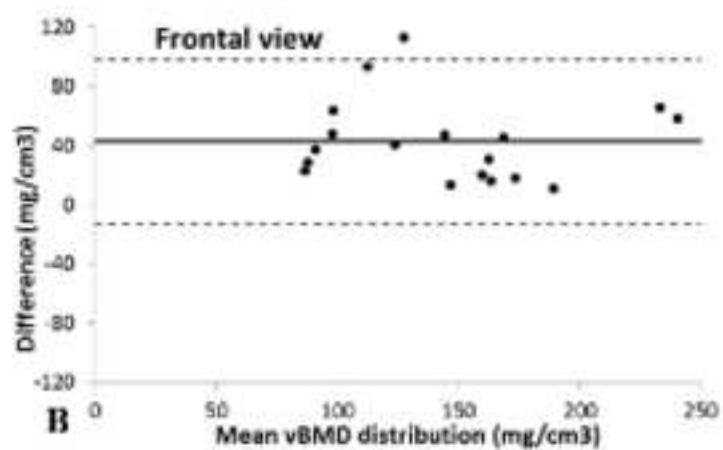
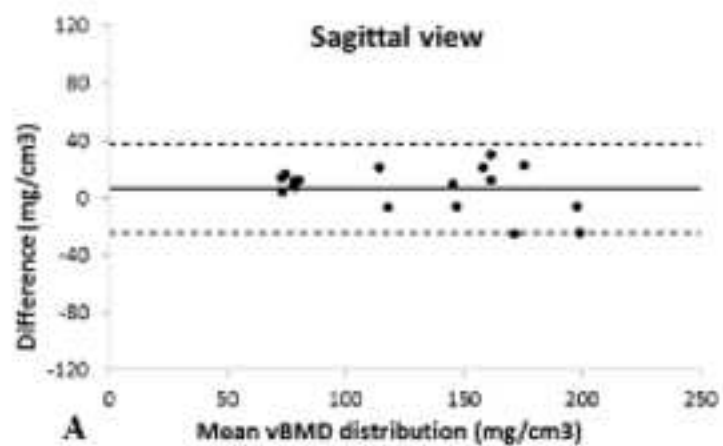


Figure4

